Proceedings of the 28th IEEE
EMBS Annual International Conference
New York City, USA, Aug 30-Sept 3, 2006

Framework for Creating New Discriminats for Detecting DTI properties: DTI Mapper

Koji Sakai*, Naohisa Sakamoto*, Jorji Nonaka*, Yukio Yasuhara, and Koji Koyamada*
Member, IEEE

Abstract— **We have commonly employed medical images, not including X-ray photography, which have their image enhanced by taking advantage of certain characteristics of the human body to look for some valuable medical information. In general, the medical imaging modalities have employed an image acquisition method which enhances a certain feature of the seat of a disease for later processing of the acquired images. Typical examples of the feature enhancement for medical images are the active area mapping on fMRI using Statistical Parametric Mapping (SPM), and the diffusivity mapping on Diffusion Tensor Imaging (DTI) using Fractional Anisotropy (FA), Apparent Diffusion Coefficient (ADC) or Relative Anisotropy (RA). Especially in DTI, many researchers have been trying to reveal the current state of a disease without any invasion of the body by using some variable discriminants. In this paper, we propose a framework, which supports and promotes the creation of new discriminants for DTI. The proposed system enables the users to create new discriminants by using eigen values from the voxels of DTI data, and to search for important clinical information applying discriminant mapping to the DTI slice images.**

I. Introduction

Some discriminants for identifying clinical feature information in Diffusion Tensor Imaging (DTI) such as the Fractional Anisotropy (FA) [1] and Apparent Diffusion Coefficient (ADC) [2] have commonly been used in daily routine work for image diagnoses. In this paper, we present a framework named "DTI-Mapper" which supports the creation of new discriminants for DTI. Although there already exist some discriminants such as FA, ADC, RA[3], VR[4] and Am[5], we believe that there are other potential discriminants which can assist and facilitate typical clinical diagnoses. Our proposed framework enables the users to create new discriminants by using eigen values from DTI data, and to search for clinical features by using slice mapping. Users can therefore create and evaluate their own discriminants interactively by using our proposed framework. Furthermore, this framework does not need eigen decomposition to obtain the existing discriminants [6] such as FA, ADC, RA, VR, and Am. As a result, the users can obtain the existing discriminants for DTI faster than using traditional eigen decomposition process.

Manuscript received April X, 2006. This research was partially supported by the Japanese Ministry of Education, Science, Sports and Culture, Grant-in-Aid for Young Scientists (B) 17700293.

Koji Sakai is with Kyoto University, Kyoto, JAPAN (corresponding author to provide phone: +81-75-753-9372; fax: +81-75-753-9365; e-mail: sakai@ kudpc.kyoto-u.ac.jp).

The remainder of this paper consists as follows: In section 2, we present the "DTI-Mapper" in more detail. We present our proposed new discriminants for detecting degenerate points in DTI in section 3. Section 4 describes the experimental subjects (digital phantom and healthy human brain) and methods. We will show some experimental results and discuss the feasibility of our approach in section 5. Finally, we summarize our method and briefly discuss future works in section 6.

II. DTI Mapper

A. Discriminants

Descriminants have been employed the feature of tissues and the seat of a disease by mapping onto a DTI slice image. Discriminants are normally obtained from acquired image intensities. In the case of Diffusion Tensor Imaging (DTI), the eigen values and corresponding eigenvectors such as FA and ADC have usually been employed because of the utilization of water diffusion property on a region of interest (ROI). In our framework, users can create their own discriminants and map them onto DTI slice images. In addition, we employed a discriminant calculation method which does not need any eigen decomposition. The details of the proposed framework (DTI-Mapper) are described in the following sections.

B. Operation

DTI-Mapper enables the users to create new discriminants through the following procedures. Figure 1 shows the outline of the process sequence in the DTI-Mapper.

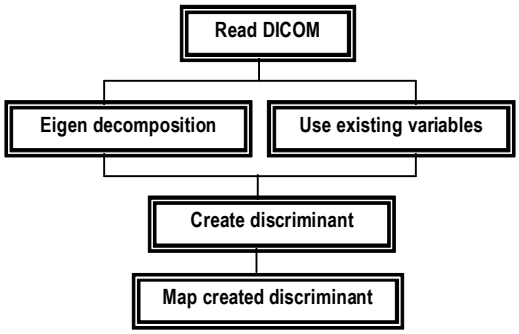

Fig.1. Outline of the process flow in DTI-Mapper

1) Read DICOM format data set

DTI-Mapper can read traditional DICOM format data. In the case of DTI, DTI-Mapper works with DTI datasets composed of normally obtained slice added with slices obtained from six different directions (green balls in Figure 2). Users can easily load their DTI data by using an intuitive user interface (Figure 2).

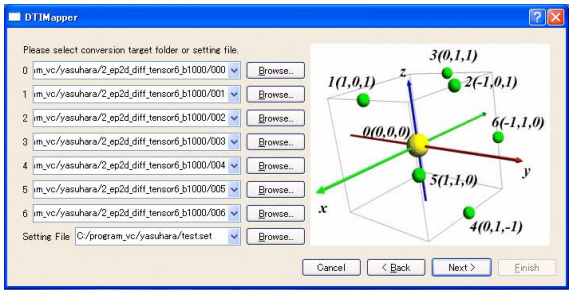

Fig.2. The user-interface for reading DTI data

2) Eigen decomposition or using existing variables

Users can select between eigen decomposition of input tensor matrix or the use of some existing variables and discriminants such as FA, ADC, RA, VR, Am (discriminants) and *P*, *Q*, and *R* (variables)(detailed in section 3.1).

DTI-Mapper calculates the tensor elements for each voxel of DTI data based on the following equation (1) [7],

$$S = S_0 e^{-bD} \qquad (1)$$

where S_0 is a non-diffusion weighted measurement signal intensity, b is the weighting factor. The eigen values are obtained by executing the eigen decomposition of matrix D. In this paper, we have used a real 3×3 symmetric tensor as the diffusion matrix.

3) Discriminant creator

Users can utilize stored discriminants or create their own through the user interface shown in Figure 3. In the latter case, users can create new discriminants by combining the eigenvalues ($\lambda max \geq \lambda mid \geq \lambda min$) and the basic arithmetic operators (+, -, *, /) and some other numerical operators (sin, cos, tan, log, exponent, squrt, pow). In addition, DTI-Mapper enables the users to create discriminants from pseudo-DTI data such as digital phantoms (detailed in section 4.1).

4) Discriminant mapping on b0 image

Users can map existing discriminants by selecting them or newly created discriminants on a *b*0 image (non-diffusion weighted measurement image) in order to execute clinical exploration about the situation of the given subject (Figure 4). DTI-Mapper uses one pop-up window for one discriminant and allows the user for selecting the desired color mapping by using the sliding bar. Users can open several pop-up windows at the same time which greatly facilitate the comparison or selection of favorable discriminants.

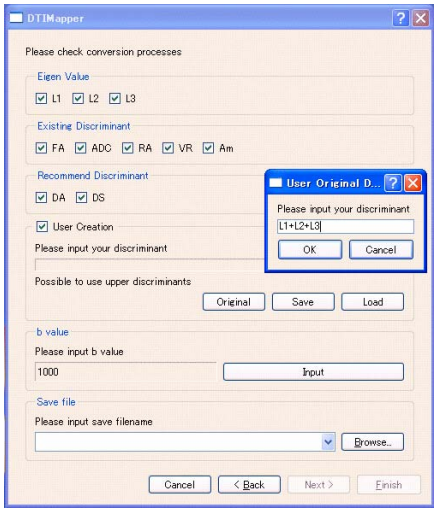

Fig.3. User-interface for selecting/creating discriminants

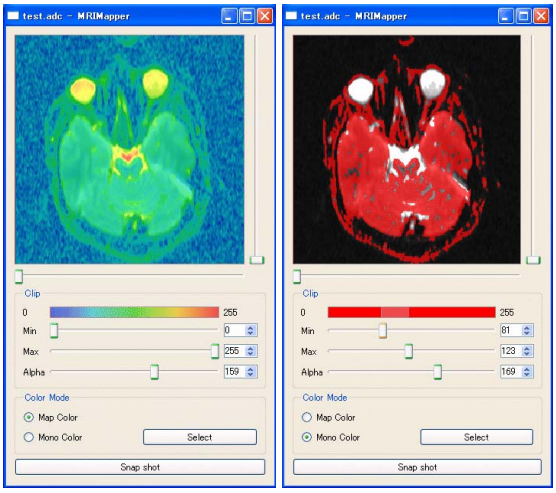

(a) color mapping (b) monotone mapping

Fig.4.Examples of discriminant mapping; (a) color, (b) monotone

Users can select the mapping range and also the color adjustment through the user-interface (in Figure 5).

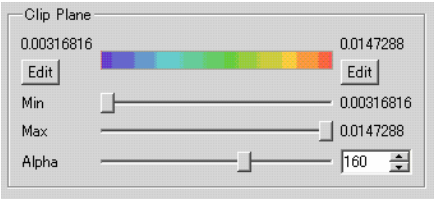

Fig.5. User-interface for selecting the range of discriminant

Furthermore, our system can simultaneously operate the slice selection of the opened discriminant pop-up windows by activating the synchronous slider check box in the control panel (DTI Mapper main panel of mapping) (Figure 6). Users can therefore observe the inter-slices changing between selected discriminants. Additionally, the level and width of each image can be changed simultaneously through the level and width sliders.

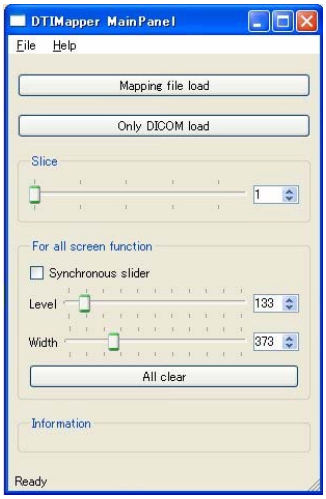

Fig.6. The main panel used for controlling the data mapping

III. NEW DISCRIMINANTS

We have already proposed two new discriminants [6] to detect diffusion degenerate points which cause the "crossing-fiber problem"[8]. The proposed two discriminants named *DA* and *DS* can reliably detect double and triple tensor degenerate points, respectively. The details of *DA* and *DS* are described in the following sections.

A. Double tensor degenerate discriminant: DA

The characteristic equation of diffusion tensor matrix can be described as shown below in equation (2).

$$F(\lambda) = \lambda^3 - P\lambda^2 + Q\lambda - R = 0 \quad (2)$$

P, *Q*, and *R* correspond to the tensor elements described below in equation (3).

$$P = D_{xx} + D_{yy} + D_{zz}$$

$$Q = \begin{vmatrix} D_{xx} & D_{xy} \\ D_{yx} & D_{yy} \end{vmatrix} + \begin{vmatrix} D_{yy} & D_{yz} \\ D_{zy} & D_{zz} \end{vmatrix} + \begin{vmatrix} D_{zz} & D_{zx} \\ D_{xz} & D_{xx} \end{vmatrix} \quad (3)$$

$$R = \begin{vmatrix} D_{xx} & D_{xy} & D_{xz} \\ D_{yx} & D_{yy} & D_{yz} \\ D_{zx} & D_{zy} & D_{zz} \end{vmatrix}$$

Our proposed method works by specifying the degeneration of diffusivity by using the relationships between the solutions and coefficients of twice differentiated equation (2) with respect to λ. Equation (4) represents the twice-differentiated equation (2) with respect to λ.

$$\lambda_i = \frac{1}{3}P \quad (4)$$

We can obtain *DA* by substituting the equation (4) in equation (2).

$$DA = -\frac{2}{27}P^3 + \frac{1}{3}QP - R \quad (5)$$

In equation (5), when $DA > 0$, the largest eigenvalue (λ_1) and the second largest eigenvalue (λ_2) are equal. In other words, this tensor represents a planar anisotropic diffusion. When $DA < 0$, the second largest eigen value (λ_2) and the smallest eigen value (λ_3) are equal, and represents linear anisotropy. By utilizing this method, *DA* can be obtained faster than other methods which employ eigen decomposition.

B. Triple tensor degenerate discriminant: DS

We have presented a new triple degenerate tensor discriminant *DS* for reliable determination of triple degenerate points and it can be described as shown below in equation (9).

$$DS = (\lambda_1 - \lambda_2)^2 + (\lambda_2 - \lambda_3)^2 + (\lambda_3 - \lambda_1)^2 \quad (6)$$

Equation (6) can be described as equation (7) substituting some elements described in the equation (4). This can be done, if and only if, all eigenvalues of equation (3) are equal and the value of *DS* is zero. It is worth noting that, *DS* also does not need any eigen decomposition as *DA*.

$$DS = 2P^2 - 6Q \quad (7)$$

IV. SOME EXPERIMENTS

A. Materials

1) Digital phantom

Table 1 shows the values at the coordinate positions for the utilized digital phantom. The origin is placed in the center of with cube composed by 27 voxels (voxel No.13). Each voxel is a cube with normalized edge length. The tensor in each voxel is modeled as being around the "crossing-fiber point". The ellipsoids in each voxel illustrate the magnitude of eigen values and the orientation of corresponding eigen vectors. Only the ellipsoid defined at the origin is a triple degenerate tensor. In Table 1, we show the eigen values, normalized eigen vector of the largest eigen value and the FA value of each voxel.

Table 1. Tensor properties

	coordinate			eigen value			emax(x,y,z)				
No.	X	Y	Z	λ1	λ2	λ3	(x	y	z	)	FA
0	−1	−1	−1	2.4	1.0	1.0	(1	1	1	)	0.839
1	0	−1	−1	2.4	1.0	1.0	(0	1	1	)	0.839
2	1	−1	−1	2.4	1.0	1.0	(−1	1	1	)	0.839
3	−1	0	−1	2.4	1.0	1.0	(1	0	1	)	0.839
4	0	0	−1	2.4	1.0	1.0	(0	0	1	)	0.839
5	1	0	−1	2.4	1.0	1.0	(−1	0	1	)	0.839
6	−1	1	−1	2.4	1.0	1.0	(1	−1	1	)	0.839
7	0	1	−1	2.4	1.0	1.0	(0	−1	1	)	0.839
8	1	1	−1	2.4	1.0	1.0	(−1	−1	1	)	0.839
9	−1	−1	0	2.4	1.0	1.0	(1	1	0	)	0.839
10	0	−1	0	2.4	1.0	1.0	(0	1	0	)	0.839
11	1	−1	0	2.4	1.0	1.0	(−1	1	0	)	0.839
12	−1	0	0	2.4	1.0	1.0	(1	0	0	)	0.839
13	0	0	0	1.0	1.0	1.0	(0	0	0	)	0.000
14	1	0	0	2.4	1.0	1.0	(−1	0	0	)	0.839
15	−1	1	0	2.4	1.0	1.0	(1	−1	0	)	0.839
16	0	1	0	2.4	1.0	1.0	(0	−1	0	)	0.839
17	1	1	0	2.4	1.0	1.0	(−1	−1	0	)	0.839
18	−1	−1	1	2.4	1.0	1.0	(1	1	−1	)	0.839
19	0	−1	1	2.4	1.0	1.0	(0	1	−1	)	0.839
20	1	−1	1	2.4	1.0	1.0	(−1	1	−1	)	0.839
21	−1	0	1	2.4	1.0	1.0	(1	0	−1	)	0.839
22	0	0	1	2.4	1.0	1.0	(0	0	−1	)	0.839
23	1	0	1	2.4	1.0	1.0	(−1	0	−1	)	0.839
24	−1	1	1	2.4	1.0	1.0	(1	−1	−1	)	0.839
25	0	1	1	2.4	1.0	1.0	(0	−1	−1	)	0.839
26	1	1	1	2.4	1.0	1.0	(−1	−1	−1	)	0.839

2) Subject: Human brain

In this paper, we focused on DTI of human brain as a subject. The data was obtained from a voluntary healthy male (23 years old) with informed consent.

B. Method

1) MR acquisition

Our data were acquired by using a SIEMENS MR Scanner (1.5 Tesla). Imaging parameters were: data size of 230mm×230mm×2.5mm, pixel size of 0.898mm×0.898mm, acquisition matrix of 256×256, diffusion direction of 6, and *b* value =1,000 s/mm^2. In addition, Spin Echo (SE) method with TR=5900ms, TE=78ms was employed.

2) Computational environment

We verified our proposal by comparing the computational times and visualization results between the synthetic tensor (digital phantom) and DT-MRI (human brain) data by using commodity computational environment (CPU: Intel® Pentium®M 1.20GHz, RAM: 0.99GB, OS: Windows XP Professional version 2002).

V. Results and Discussions

A. Digital phantom

Figure 7 shows the computation results of FA values obtained from Table 1. In this figure, the dashed lines and the numbers were added by the authors for easy understanding. The color-patch (rectangular pixels) was provided by the DTI-Mapper. The colors correspond to the FA values. The highest value is assigned the red color, the lowest value is assigned the blue color, the intermediate colors obey the color chart shows in Figure 7.

From this figure, we can verify that DTI Mapper can correctly calculate FA values and map them on the corresponding-pixels. We also obtained correct results from other discriminants, including user created discriminants such as *DA* and *DS*.

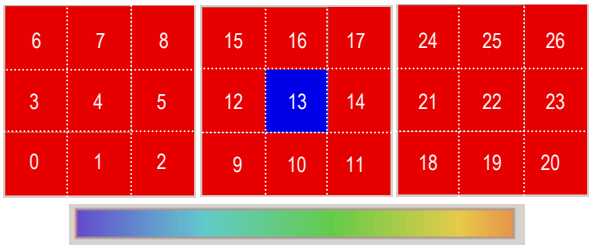

Fig.7. The results of the digital phantom analysis

B. Human brain

Mapping results for existing discriminants FA, ADC, and our proposed disctriminants *DA* and *DS* on the subject human brain are shown in Figure 8. These figures show a slice near to the corpus callosum. Figure 8(a) shows the contour mapping of FA values. Values from the minimum to the maximum are mapped to colors ranging from blue to red (same as the color bar shows in Figure 7). In this figure, FA values of splenium of corpus callosum and genu of corpus callosum are higher than other parts. The reason for this is the distribution of large fiber bundles. Figure 8(b) shows an example of an ADC value which can depict anisotropic tensor diffusion area such as the boundary of gray matter (GM) and white matter (WM) and ventricle. Figure 8(c) represents the *DA* value by using the same color mapping. We can verify that the whole area, excepting GM and ventricle areas can be well depicted when using *DA*. In this case, the aerial area around the brain is depicted as being WM region. For practical use however, *DA* must have the dynamic range improved. Figure 8(d) represents the area with *DS* ranging from 0.0 to 0.01. We can verify that Figure 8(d) can show the boundary regions between GM, WM, ventricle and other areas more clearly than Figure 8(b).

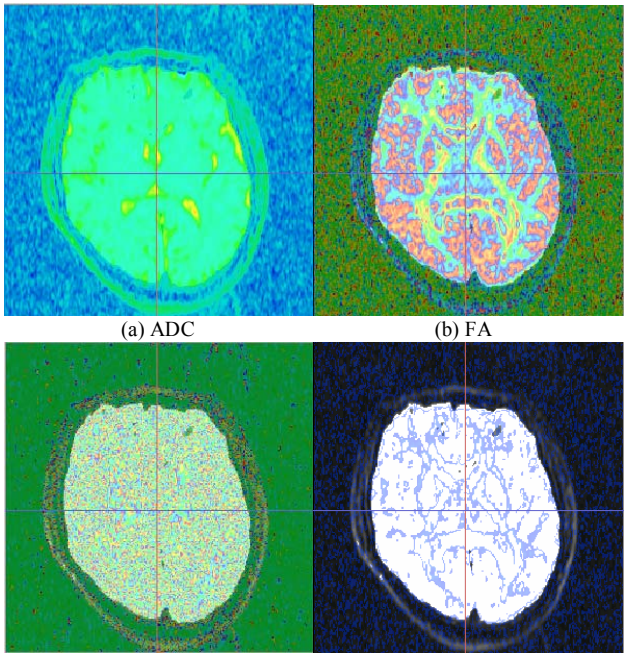

(a) ADC (b) FA

(c) DA (d) DS

Fig.8. Degeneracy visualization of DT-MRI data

C. Computation time

Figure 9 shows the computation time for obtaining the eigen values and the discriminants for human brain DTI data set with and without using eigen decomposition. From Figure 9, we can verify that our proposed method is approximately ten times faster than the traditional methods which employ eigen decomposition. In Figure 9, "eigen value" means the three eigen values, which are obtained from eigen decomposition of a tensor matrix *D*. We believe that when the number of DTI datasets which require at least one data analysis become large then the proposed method which does not require eigen decomposition becomes extremely attractive regarding computational cost.

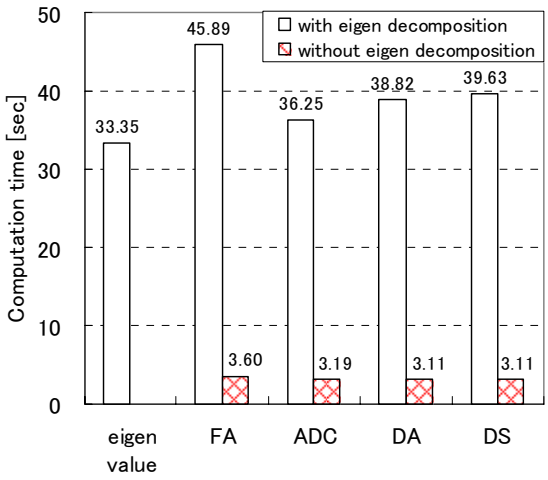

Fig.9. Computation time of eigen values and discriminants

VI. Conclusion

Our proposed system allows to speeding up computation time of existing discriminants. In addition, our proposed system enables the users to create, study, and evaluate their own discriminants. We also presented our new discriminants, named *DA* and *DS*, for detecting some degenerate diffusion properties.

We expect to expand our framework for other MR modalities such as Magnetic Resonance Imaging (MRI), functional MRI, and Perfusion Weighted Imaging (PWI) in our future work. We are also planning to provide this framework for the researchers who are involved in clinical works or medical science.

Acknowledgement

We are deeply grateful to Dr. Kei Yamada (Kyoto Prefectural University of Medicine) for his useful comments and discussions from the clinical point of view. We also thank our colleagues in Koyamada Laboratory at Kyoto University for their support during this work.

References

[1] Basser P.J., Pierpaoli C., "Microstructual and physiological feature of tissues elucidated by quantitative diffusion tensor MRI," *Journal of Magnetic Resonance series B*, 1996, 111, pp.209-219

[2] Taylor D.G., Bushell M.C., "The spatial mapping of translational diffusion coefficients by the NMR imaging technique." *Physics in medicine and biology*, 1985, 30, pp.345-349

[3] Basser P.J., Pierpaoli C., "A simplified method to measure the diffusion tensor from seven MR images," *Magnetic Resonance in Medicine*, 1998, 39, pp.928-934

[4] Pierpaoli C., Basser P.J., "Toward a quantitative assessment of diffusion anisotropy," *Magnetic Resonance in Medicine*, 1996, 36, pp.893-906

[5] van Pul C., Buijs J., Janssen M. J. A., Roos G. F., Vlaardingerbroek M. T., and Wijn P. F. F, "Selecting the Best Index for Following the Temporal Evolution of Apparent Diffusion Coefficient and Diffusion Anisotropy After Hypoxic-Ischemic White Matter Injury in Neonates," *American Journal of Neuroradiology*, 2005, 26, pp.469-481

[6] Sakai K., Koyamada K., "New Discriminants for Detecting Degenerate Areas in DT-MRI", *In Proceedings of the 4th IASTED International Conference on Biomedical Engineering* (BioMED) 2006, Feb 15-17, Innsbruck, Austria, pp.200-205.

[7] E.O.Stejskal and J.E.Tanner, "Spin diffusion measurements: spin echoes in the presence of a time-dependent field gradient", *Journal of Chemical Physics*, 42, pp.288-292, 1965.

[8] M. Kinoshita, K. Yamada, N. Hashimoto, A. Kato, S. Izumoto, T. Baba, M. Maruno, T. Nishimura, and T. Yoshimine, "Fiber-tracking does not accurately estimate size of fiber bundle in pathological condition: initial neurosurgical experience using neuronavigation and subcortical white matter stimulation", *NeuroImage* 25(2005), pp.424-429